

# Torque Observer-Based Control of Self-Energizing Clutch Actuator for Dual Clutch Transmission

Jiwon J. Oh, Jeong Soo Eo, and Seibum B. Choi

**Abstract**—Using an adaptive sliding mode control scheme based on the dual clutch torque observer, this brief proposes a novel strategy to control the clutch engagement for the dual clutch transmission (DCT) equipped with the self-energizing clutch actuator. The contribution of this brief is twofold. A sliding mode tracking controller for the actuator motor position is developed by using the information provided by the torque observer designed to estimate the torque transferred through each clutch of the DCT. Then, the adaptive strategy to actively alter the target position command to compensate for the model uncertainty or disturbance is proposed. The actuator position tracking control accuracy improvement attained by using the adaptive sliding mode controller and, most crucially, the ability for the integrated controller to cope with the system disturbance are verified in an integrated manner via actual experiments using the driveline test bench.

**Index Terms**—Clutch actuator, driveline, dual clutch transmission (DCT), torque-tracking control, vehicle.

## I. INTRODUCTION

**D**UE TO THE scarcity of energy and the environmental issues, the needs for improving the vehicle powertrain efficiency by replacing the hydraulic coupling by physical engagement [1]–[4] have increased, and the dual clutch transmission (DCT) [5] has been gaining popularity. With carefully designed clutch actuator control methods for DCTs to optimize the clutch slip and shift jerk [6], [7], the fuel economy similar or higher than that of the manual transmission can be reached, as well as the convenience of automatic gear shifts for the driver and potential for further modification, such as hybridization of powertrain [8]–[11].

The weakness of the conventional DCT, however, is in the actuator. To ensure satisfactory control performance of the clutch engagement force by reducing the sensitivity of the engagement force variation, diaphragm springs are installed in the dry-type clutch package [2]. This works against the

actuation efficiency by leading to higher energy consumption in the clutch actuator via having to travel through longer displacement to reach the desired engagement force.

As a resolution for this issue, this brief selected the control target as the self-energizing clutch actuator (SECA), which replaces the diaphragm spring in a conventional dry-clutch system [6]. Here, the torque-monitoring control methodology is proposed to overcome the system's oversensitivity. Such combination can lead to both clutch actuation efficiency improvement and shift quality improvement in addition to the benefits of the conventional DCTs.

Actuator controllers designed in most of the previous efforts take the form of pure position-based control [2], [6], [12], [13]. However, the consistency in tracking performance can be severely degraded due to the deviation of the system parameter from the nominal values, such as variation in the friction property or elasticity constant of the hardware [14], especially for the system in which diaphragm spring is eliminated [6]. The influence of clutch wear and thermal variation may also contribute to the uncertainty [15], [16].

As an alternative, strategies to control the clutch based on the clutch slip information have been previously developed as well [7], [17]–[19]. However, such method still is unable to track the desired torque under the influence of load torque disturbances, and to monitor the torque transferred through both each clutch in the driveline with DCT. Also, their rule-based control strategies are overly generalized.

Model-based control methods are proposed as well. However, the controller is built based on the ideal assumption about the model accuracy [20], and it largely depends on the offline identification of the clutch's torque transmissibility table [21], [22].

So this brief suggests an adaptive method for the torque-tracking control by making use of the dual clutch torque observer, which was developed in [23]. The main contribution of this brief is the design of controller with the improved clutch transferred torque tracking ability when error exists in the clutch friction parameter. This brief also provides the theoretical and empirical analysis of the closed-loop system consisting of the observer and controller.

The contents are organized as follows. Section II first describes the control target. Section III provides details on the controller algorithm, which includes the kissing point identification, position tracking controller, and adaptive scheme for torque-tracking control. In Section IV, the experiment results for each algorithm introduced in Section III are discussed, as well as the test bench experiment results obtained by using the integrated controller. Through testing the performance of the proposed actuator controller, the torque tracking ability

Manuscript received April 12, 2016; revised June 21, 2016; accepted October 16, 2016. Date of publication November 9, 2016; date of current version August 7, 2017. Manuscript received in final form October 20, 2016. This work was supported in part by the MSIP Ministry of Science, ICT and Future Planning, Korea, under the ITRC Information Technology Research Center support program Grant IITP-2016-H8601-16-1005 supervised by the IITP Institute for Information & communications Technology Promotion, the BK21 plus program, and the National Research Foundation of Korea (NRF) grant funded by the Korea government (MSIP) Grant 2010-0028680. Recommended by Associate Editor E. Usai. (*Corresponding author: Seibum B. Choi.*)

J. J. Oh and S. B. Choi are with KAIST, Daejeon 34141, South Korea (e-mail: jwo@kaist.ac.kr; sbchoi@kaist.ac.kr).

J. S. Eo is with Hyundai Motor Company, Hwaseong 18280, South Korea (e-mail: fineejs@hyundai.com).

Color versions of one or more of the figures in this paper are available online at <http://ieeexplore.ieee.org>.

Digital Object Identifier 10.1109/TCST.2016.2620421

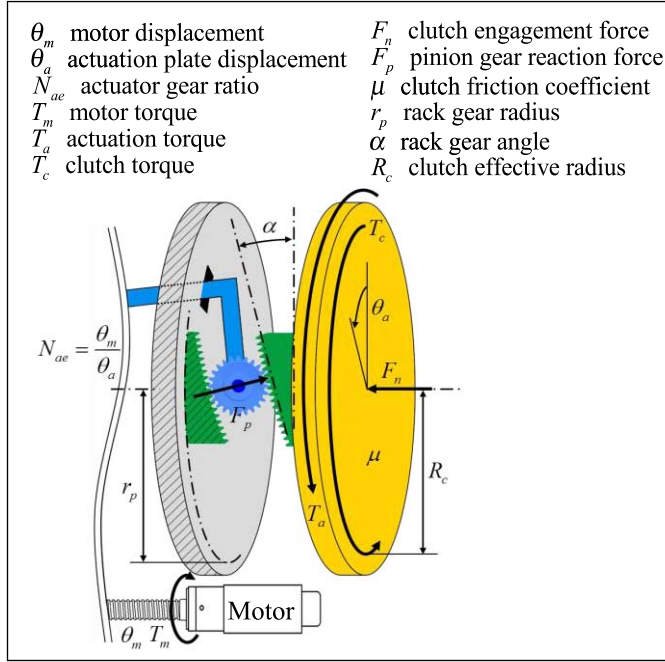


Fig. 1. SECA model.

in the presence of the vast range of model uncertainty is experimentally verified.

## II. SYSTEM DESCRIPTION

### A. Self-Energizing Clutch Actuator

The self-energizing actuator refers to the mechanism designed, so that the actuation effort is facilitated by itself. In other words, when the actuator exerts force to the clutch in the engaging direction, the actuation mechanism is intentionally designed, so that the driving torque acting on the clutch adds to the actuation effort. Such principle has been applied not only to the clutch actuation [6], [13], but also to wedge brakes [24]–[26] and drum brakes [27], [28] as well.

The basic working principle of the SECA used for this brief is as shown in Fig. 1. As illustrated, an electric motor is designed to turn the pinion gear by pushing onto it. Since the pinion gear is interlocked between a pair of inclined rack gears, rotation of the pinion gear induces both angular and linear displacement of the pressure plate relative to the actuator housing. Such motion causes the pressure plate to press onto the friction clutch, while the torque transferred by the clutch disk is exerted onto the pressure plate, providing the self-energizing torque.

The torque balance equation for the above-shown pressure plate is as follows:

$$J_a \ddot{\theta}_a = \begin{cases} T_a - T_f, & \text{when disengaged} \\ T_a + T_c - 2r_p F_p \sin \alpha - T_f, & \text{when in contact.} \end{cases} \quad (1)$$

Here,  $J_a$  is the equivalent inertia from the perspective of the pressure plate, and  $T_f$  is the sum of the friction torque in the actuation route, which acts on the pressure plate.

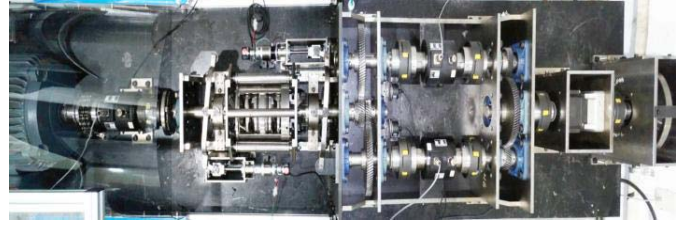


Fig. 2. Test bench driveline.

Also, the relationship between the clutch normal force and the pinion gear reaction force is as follows:

$$F_p = \frac{F_n}{\cos \alpha}. \quad (2)$$

Using (1) and (2), the mechanical dynamics of the actuator motor can be expressed as follows:

$$J_a^* \dot{\omega}_m = \begin{cases} T_m - T_f^*, & \text{when disengaged} \\ T_m + \frac{T_c}{N_{ae}} - \frac{2r_p \tan \alpha}{N_{ae}} F_n - T_f^*, & \text{when in contact} \end{cases} \quad (3)$$

where  $T_f^*$  indicates the sum of the friction torque in the actuation route, which acts on the motor, and

$$J_a^* = \frac{J_a}{N_{ae}^2}. \quad (4)$$

Now, the electrical part of the motor is modeled simply as

$$L_m \frac{di_m}{dt} = -k_{emf} \omega_m - R_m i_m + u_m \quad (5)$$

$$T_m = k_q i_m \quad (6)$$

where  $L_m$ ,  $k_{emf}$ ,  $k_q$ ,  $R_m$ ,  $i_m$ , and  $u_m$  are the motor inductance, back-emf constant, torque constant, armature resistance, motor current, and control input (the armature voltage of the dc motor), respectively. The friction acting on the motor is modeled with LuGre friction model [29].

### B. Dual Clutch Transmission Driveline Test Bench

The driveline test bench is constructed to test the performance of the developed controller. Main components of the test bench, including the ac motor, dual clutch and their actuators, transmission gears, torque sensor, output shaft, and the load, are shown in Fig. 2.

Here, the role of the engine is played by an ac motor. Similar to the case of an actual vehicle powertrain with dual mass flywheel, the drive torque of the engine is transferred to the clutches through an external damper to reduce torsional vibration. The clamping forces in a pair of coaxially positioned clutches determine the transmission of torque onto each transfer shaft. Such torque is amplified by the transmission gears and final reduction gears. Fixed gear ratios of different values are applied to each transfer shaft. The total reduction gear ratio from engine to wheel is 18 for the first gear and 11.52 for the second gear. Finally, the transfer shaft torques are transmitted to the output shaft to exert torque onto the wheels and the vehicle load. To obtain the driveline speeds, speed measurement sensors are attached directly on

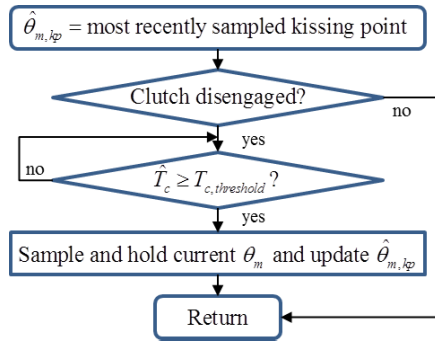


Fig. 3. Kissing point identification logic.

the ac motor, actuator motors, transfer shafts, and output shaft. Also, only for validation purpose, torque measurement sensors are installed in the ac motor shaft and transfer shafts.

### III. CONTROLLER ALGORITHM

The control architecture consists of four major parts: dual clutch torque observer [23], kissing point identification, actuator tracking controller, and adaptive target position correction. The major role of the torque observer is to provide accurate estimation of the torque transferred through each clutch for the rest of the parts in the controller algorithm.

Based on this torque information, the feedforward accuracy is majorly improved in the sliding mode position tracking controller designed for the actuator motor, since the magnitude of the self-energizing effect can be identified. Also, the estimated torque information utilized in the adaptive target position correction enables the torque-tracking control even under the influence of clutch parameter uncertainty.

#### A. Kissing Point Identification

Before presenting the main contribution on the clutch controller, the kissing point identification process that calibrates the actuator position value to maintain consistent control performance must be introduced. The main reason for such calibration is to deal with the long-term change in clutch thickness due to its wear that occurs from repeated slippage possibly during traffic congestion and uphill launch.

Using the torque estimation [23] provides an advantage in identifying the kissing point. Its basic idea, shown in Fig. 3, is to sample the current actuator motor position  $\theta_m$  at the moment the estimated clutch torque exceeds the predefined threshold  $T_{c,threshold}$  during the clutch engagement phase, and set this value as the newly updated kissing point,  $\hat{\theta}_{m,kp}$ . To ensure that such process takes place only during the engagement phase for consistency, it must be checked whether the clutch has been disengaged before sampling, as shown in the second line in Fig. 3. Any value of  $T_{c,threshold}$  within the range of clutch torque capacity would be suitable as long as the sampled kissing points are consistent in magnitude, but it should be fairly large to avoid oversensitivity issue due to noise. The selected parameter is shown in the Appendix.

Here, the clutch kissing point can be considered slowly varying, because the overall thickness change in the clutch

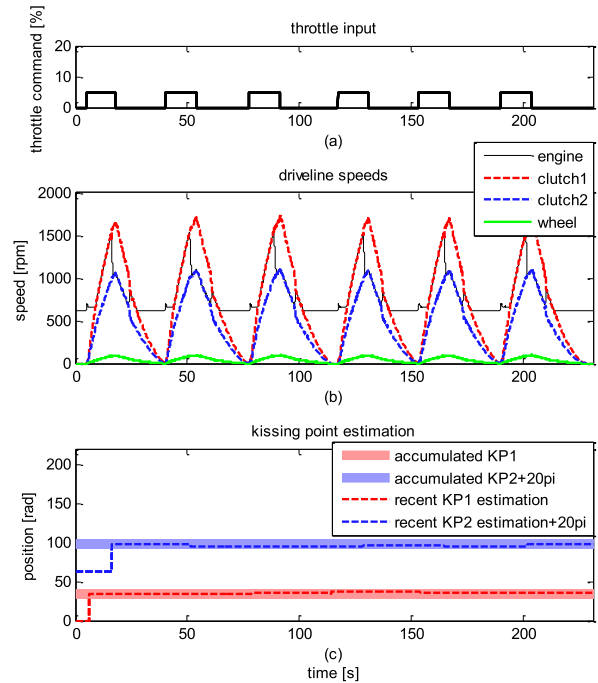


Fig. 4. Kissing point identification experimental results. (a) Throttle input. (b) Driveline speeds. (c) Kissing point estimation.

due to wear happens over an extended period of time. Hence, the mean value of predefined number of previously identified samples can be considered as the kissing point for real vehicle application, so that possible error due to noise and disturbance can be rejected.

The kissing point estimation procedures are described in terms of general states without distinguishing between clutches 1 and 2. Please note that the above-mentioned terms can be equivalently applied to the kissing point estimation of either clutch. The kissing point identification experiments are conducted while the engine is running, since the estimation algorithm is based on the torque-monitoring tactics.

As shown in Fig. 4, kissing point of each clutch is effectively identified by using the suggested algorithm, and the estimated values are consistent over repeated trials. The variation in the final result of the identified kissing point obtained this way turned out to be less than 2% of the entire clutch wear range, and such performance can be considered sufficient for the long-term wear compensation.

#### B. Actuator Tracking Controller

Before considering the accurate torque-tracking performance of the controller, it must first be able to accurately track the desired actuator position, so that further correction for improved torque-tracking performance can be achieved with the adaptive scheme.

The actuator position tracking error is first defined as

$$\tilde{\theta}_m \equiv \theta_m - \theta_{m,d} \quad (7)$$

where  $\theta_{m,d}$  is the desired motor position.

It must be noted here that this section only shows the design process of the controller for a single actuator.

The design process of the controller for the second actuator is omitted, since it is analogous to that of the first.

Now, the sliding surface is defined as follows:

$$s = \dot{\theta}_m + \lambda \bar{\theta}_m \quad (8)$$

where  $\lambda$  is a positive constant. Using this sliding surface, the following desired motor current is calculated:

$$i_{m,d} = \frac{\hat{T}_f^*}{k_q} - \frac{\hat{T}_c}{k_q N_{ae}} + \frac{2r_p \tan \alpha}{k_q N_{ae}} \hat{F}_n + \frac{J_a^*}{k_q} \ddot{\theta}_{m,d} - \frac{J_a^* \lambda}{k_q} \dot{\theta}_m + \frac{J_a^* \lambda}{k_q} \dot{\theta}_{m,d} - \frac{J_a^* \gamma_s}{k_q} \text{sat} \left( \frac{s}{\Phi} \right). \quad (9)$$

Here,  $\gamma_s$  is the sliding gain,  $\Phi$  is the factor for determining the smoothing domain for the signum function, and  $\text{sat}(\cdot)$  is the operator for saturation at  $\pm 1$ . The estimated clutch torque  $\hat{T}_c$  from the clutch torque observer is utilized to obtain the desired motor current.

The smoothing domain is applied to prevent the potential chattering issue—a critical drawback of using the sliding mode controller. Also, the use of model-based feedforward controller may deteriorate the performance when the model accuracy is not high. Hence, it must be emphasized that the clutch torque estimation is fed into the model used to design the sliding mode controller for model accuracy improvement.

For choosing the sliding gain, the following must be satisfied:

$$\gamma_s > C_v \geq \|v\|_1 \quad (10)$$

where the system uncertainty is the product of the estimation error coefficient and the estimation error vector, including the clutch torque estimation error, clutch engagement force model error, and actuator friction error, such that

$$v(t) \equiv \begin{bmatrix} \frac{1}{J_a^* N_{ae}} & -\frac{2r_p \tan \alpha}{J_a^* N_{ae}} & -\frac{1}{J_a^*} \\ \tilde{T}_c(t) & \tilde{F}_n(t) & \tilde{T}_f^*(t) \end{bmatrix}^T \quad (11)$$

whose greatest  $L_1$ -norm over all  $t$  is upper bounded by a positive constant  $C_v$  with knowing that the magnitudes of each element in  $v(t)$  are physically limited.

For the calculation of the motor voltage input, the following can be obtained by assuming that the electrical motor dynamics described in (5) holds:

$$u_m = L_m \frac{di_{m,d}}{dt} + k_{emf} \omega_m + R_m i_{m,d}. \quad (12)$$

### C. Adaptive Target Position Correction

As mentioned earlier, the sensitivity and model uncertainty related to the clutch transferred torque against actuator position is an obstacle to accurate torque-tracking control, especially in case using the SECA where diaphragm spring is eliminated for higher actuation efficiency. Hence, an adaptive scheme is developed to correct the desired motor position on real-time basis, so that desired torque can be transferred through each clutch even with disparity between the nominal clutch parameter and actual clutch parameter.

Since the torque-monitoring strategy for actuator control is meaningful in the presence of the clutch slip, the clutch torque can be described by using the slip-phase model as shown next for the sake of simplicity

$$T_c = \mu R_c F_n = \mu R_c k_c \theta_m = R_c C_c \theta_m. \quad (13)$$

Here,  $C_c \equiv \mu k_c$ , where  $k_c$  represents the effective spring constant of the clutch friction plate. Now, the above-mentioned representation of the clutch torque can be described in terms of the nominal and unknown parts, denoted by subscript “ $n$ ” and “ $u$ ”, respectively

$$T_c = R_c (C_{c,n} + C_{c,u}) \theta_m \quad (14)$$

where  $C_{c,n} \equiv \mu_n k_{c,n}$  and  $C_{c,u} \equiv \mu_n k_{c,u} + \mu_u k_{c,n} + \mu_u k_{c,u}$ . Also,  $\hat{T}_c$  and  $\tilde{T}_c$  are the known estimated clutch torque and unknown clutch torque estimation error, respectively.

Now, the unknown clutch torque estimation error is expressed using the shaft compliance model introduced in [23] as follows:

$$\tilde{T}_c = k_{t,u} (\theta_c - \theta_o i_t) \quad (15)$$

where  $k_{t,u}$ ,  $\theta_c$ ,  $\theta_o$ , and  $i_t$  are unknown part of the transfer shaft torsional spring constant, clutch shaft angular displacement, output shaft angular displacement, and effective gear ratio, respectively.

Separating the unknown terms on the left-hand side and the known terms on the right-hand side, the following equation is reached:

$$-k_{t,u} (\theta_c - \theta_o i_t) + R_c C_{c,u} \theta_m = \hat{T}_c - R_c C_{c,n} \theta_m. \quad (16)$$

From this, the internal state  $z$  for adaptation can be defined to be equal to the left-hand side of (16), and a filter with the gain of  $\gamma_z$  is applied to prevent noise sensitivity issue caused by direct calculation of the adaptive variables, which leads to the dynamics of the estimated  $z$  and adaptive laws as shown in the following:

$$\dot{\hat{z}} = -\gamma_z \hat{z} + (\gamma_z R_c \hat{C}_{c,u} \theta_m - \gamma_z \hat{k}_{t,u} (\theta_c - \theta_o i_t)) \quad (17)$$

$$\dot{\hat{C}}_{c,u} = \gamma_{a1} \gamma_z R_c \theta_m \varepsilon \quad (18)$$

$$\dot{\hat{k}}_{t,u} = -\gamma_{a2} \gamma_z (\theta_c - \theta_o i_t) \varepsilon \quad (19)$$

where  $\gamma_{a1}$  and  $\gamma_{a2}$  are the adaptive gains and  $\varepsilon = z - \hat{z}$ .

The parameters  $\hat{C}_{c,u}$  and  $\hat{k}_{t,u}$  will converge to their true values if the regressors  $\theta_m$  and  $\theta_c - \theta_o i_t$  on the right-hand sides of the adaptive laws in (18) and (19) satisfy the persistence of excitation (PE) requirement [30]. Also, adaptation algorithm is designed to perform only when (13) holds. That is, if the clutch is fully engaged and (13) is no longer valid, adaptive states are held at the most recently achieved value.

Now that the adaptive law is established, general steps for the actuator control can be described. When the desired clutch torque is given by the transmission control unit (TCU), the first step is to calculate the nominal desired position  $\theta_{m,d,n}$  for the actuator, based on (13)

$$\theta_{m,d,n} = \frac{T_{c,d}}{R_c C_{c,n}}. \quad (20)$$

Here,  $T_{c,d}$  is the desired clutch torque command generated by the vehicle TCU. Now, in order to compensate for the model uncertainty in the clutch friction coefficient and clutch disk spring constant, the nominal desired position  $\theta_{m,d}$  is obtained by rescaling  $\theta_{m,d,n}$  with the correction factor  $\eta$

$$\theta_{m,d} = \eta \theta_{m,d,n}. \quad (21)$$

The dynamics of the correction factor is described next, using a filter with the appropriate gain  $\gamma_\eta$

$$\dot{\eta} = \gamma_\eta \left( \frac{T_{c,d}}{R_c(C_{c,n} + \hat{C}_{c,u})} - \theta_{m,d} \right). \quad (22)$$

The modification of the reference position is conducted in a separate step from the adaptation, so that the adaptive identification can be completed while (13) holds, without causing the driveline oscillation induced from rigorously modifying the reference position trajectory.

Finally, the desired actuator position obtained this way is used to calculate the actuator input, based on (12).

Now select a Lyapunov function as

$$V = \frac{1}{2}\varepsilon^2 + \frac{1}{2}s^2 + \frac{1}{2\gamma_{a1}}\tilde{C}_{c,u}^2 + \frac{1}{2\gamma_{a2}}\tilde{k}_{t,u}^2 \quad (23)$$

where  $\tilde{C}_{c,u} \equiv C_{c,u} - \hat{C}_{c,u}$  and  $\tilde{k}_{t,u} \equiv k_{t,u} - \hat{k}_{t,u}$ .

Differentiating the Lyapunov function with respect to time leads to

$$\begin{aligned} \dot{V} &= \varepsilon \dot{\varepsilon} + s \dot{s} + \frac{1}{\gamma_{a1}}\tilde{C}_{c,u}\dot{\tilde{C}}_{c,u} + \frac{1}{\gamma_{a2}}\tilde{k}_{t,u}\dot{\tilde{k}}_{t,u} \\ &= -\gamma_z\varepsilon^2 + \tilde{C}_{c,u} \left( \gamma_z R_c \theta_m \varepsilon - \frac{1}{\gamma_{a1}}\dot{\hat{C}}_{c,u} \right) \\ &\quad + \tilde{k}_{t,u} \left( -\gamma_z(\theta_c - \theta_o i_t)\varepsilon - \frac{1}{\gamma_{a2}}\dot{\hat{k}}_{t,u} \right) \\ &\quad + s \left( v - \gamma_s \text{sat} \left( \frac{s}{\Phi} \right) \right) \quad \because \\ &= -\gamma_z\varepsilon^2 + vs - \gamma_s s \text{sat} \left( \frac{s}{\Phi} \right) \quad \because (18) \text{ and } (19) \\ &\leq 0 \quad \because (10), \text{ given } |s| \geq \Phi. \end{aligned} \quad (24)$$

Since  $\dot{V}$  is negative semidefinite,  $\varepsilon$ ,  $s$ ,  $\tilde{C}_{c,u}$ , and  $\tilde{k}_{t,u}$  are bounded. Now, the second derivative of the Lyapunov function with respect to time is calculated as shown in the following:

$$\ddot{V} = -2\gamma_z\varepsilon\dot{\varepsilon} + (\dot{v}s + v\dot{s}) - \gamma_s \left( \dot{s} \text{sat} \left( \frac{s}{\Phi} \right) + s \frac{d}{dt} \left( \text{sat} \left( \frac{s}{\Phi} \right) \right) \right). \quad (25)$$

With the previously obtained results and the assumption that  $\dot{v}$  is also bounded in physical sense, it can be shown that  $\varepsilon$ ,  $s$ ,  $\tilde{C}_{c,u}$ , and  $\tilde{k}_{t,u}$  converge to zero as  $t \rightarrow \infty$  by applying Barbalat's lemma [31], as long as  $\theta_m$  and  $\theta_c - \theta_o i_t$  satisfy the PE requirement [30].

#### IV. EXPERIMENT

Experiments are conducted by using actual driveline test bench to test the performance of the algorithms proposed in this brief. MicroAutobox dSPACE 1401 is used to run the control software and to process the signals from the sensors.

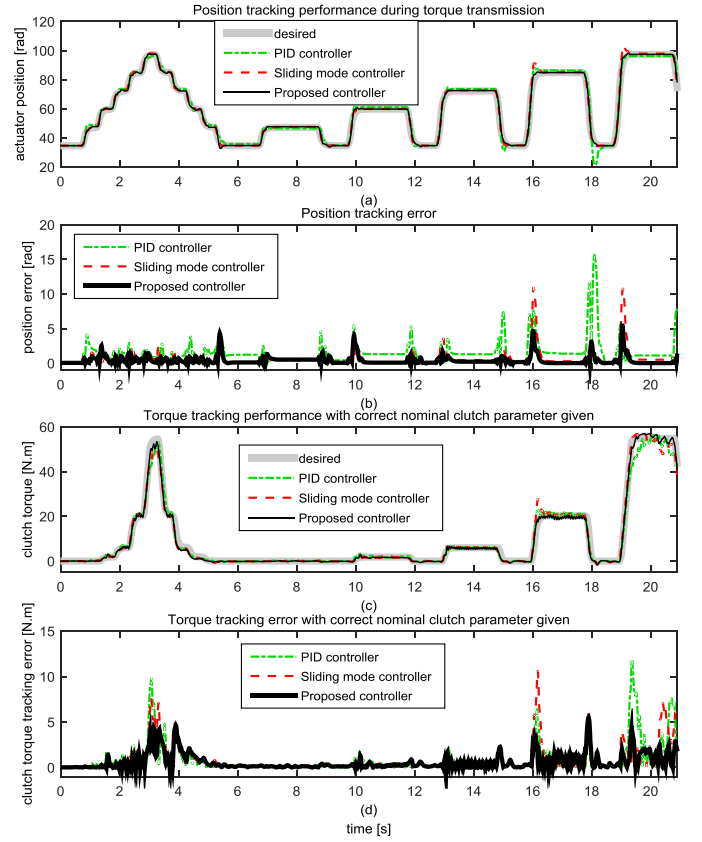


Fig. 5. Position tracking experiment results obtained by using three controllers. PID controller. Conventional sliding mode controller. Proposed sliding mode controller. (a) Position tracking performance during torque transmission. (b) Position tracking error. (c) Torque tracking performance with correct nominal clutch parameter given. (d) Torque tracking error with correct nominal clutch parameter given.

In the first part of the experiment results, the proposed actuator position tracking controller is tested and its tracking ability is compared against that shown by classical PID controller and previously published sliding mode controller. Then, as the highlight of the proposed work, the integrated torque observer-based controller system designed with adaptive scheme is tested, whose performance reflected on the driveline is displayed and analyzed.

##### A. Actuator Tracking Controller

Position tracking performance is experimentally tested using three controllers: classical PID feedback controller, predefined model-based sliding mode controller, and the proposed sliding mode controller with clutch torque estimation feedback.

To emphasize the benefit of using the model-based control methodology on top of feedback controller, position tracking performance of the proposed controller is compared first with that of the PID controller. Then, to demonstrate the importance of using the high accuracy model in the feedforward controller design, the proposed controller's performance is also compared against that obtained by the sliding mode controller without estimated clutch torque information in the control loop. Such controller whose details are found in a recently published work [6] is, henceforth, referred to as the conventional sliding mode controller.

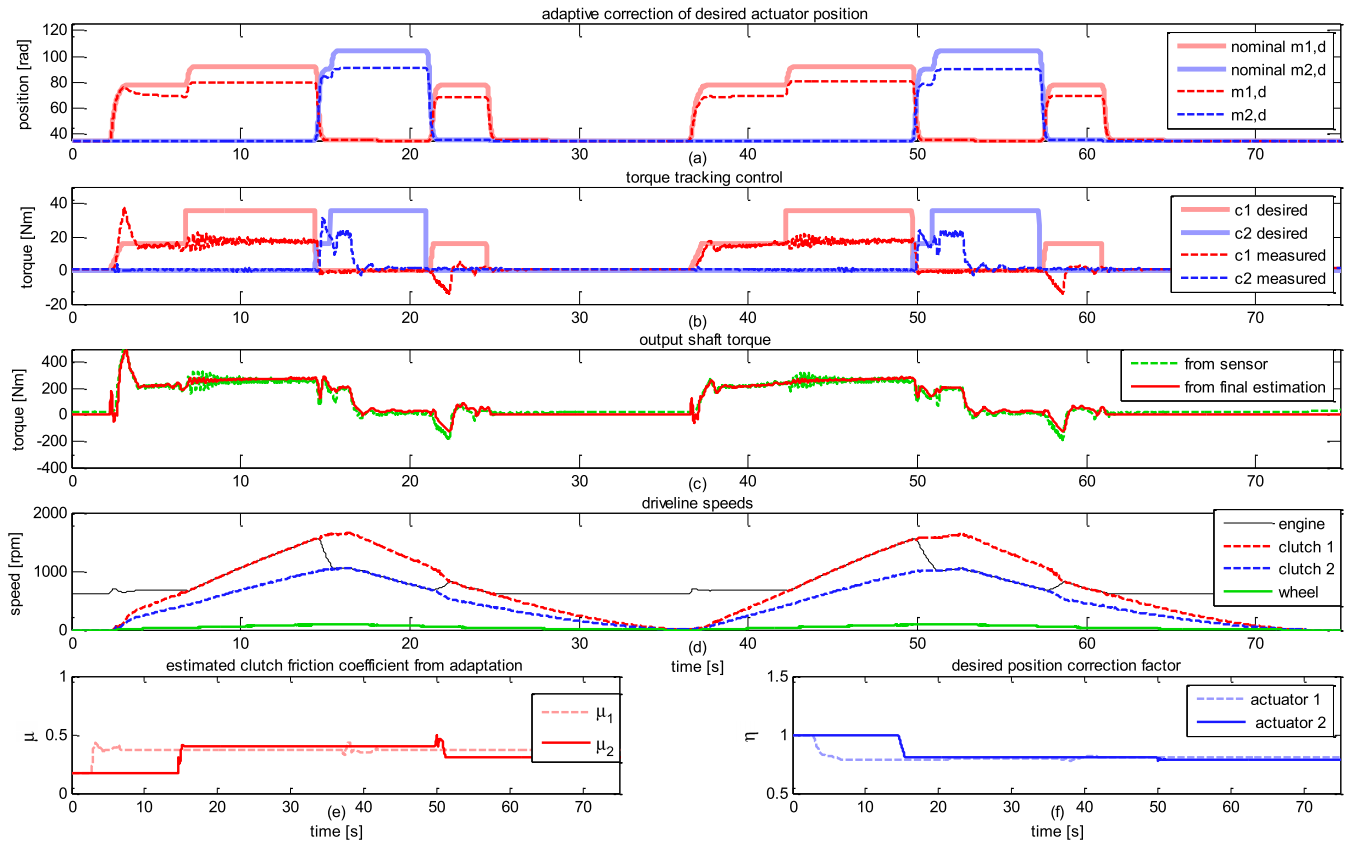


Fig. 6. Experiment results obtained by using the proposed integrated controller with underestimated clutch parameter. (a) Adaptive correction of desired actuator position. (b) Torque tracking control. (c) Output shaft torque. (d) Driveline speeds.

The conventional sliding mode controller does include the self-energizing torque term in the modeled actuator dynamics. However, since real-time estimation of the clutch torque is not available, model accuracy can be degraded in case of clutch parameter variation. Such limitation is reflected in the test results shown in Fig. 4, where the uncompensated self-energizing torque due to underestimated clutch friction coefficient causes overshoot in the actuator position during clutch engagement around 16 and 19 s. In contrast, the accurate tracking performance is maintained without any overshoot even in the existence of the clutch torque disturbance when the proposed controller is used.

Furthermore, Fig. 5(c) and (d) shows the position tracking performance in terms of torque tracking performance acquired through the position-based control method. Here, correct values of clutch parameters are used for all controllers to compare the effects of position tracking performance on the torque tracking performance. As expected, the proposed controller showed the most satisfactory tracking performance. These tracking errors are compared quantitatively in Table I. The engineering goal is to meet the tracking performance criterion of 10% error to avoid possible issue regarding shift quality and durability. The quantitative results in Table I show that the conventional controllers do not meet such criterion when the clutch torque is uncompensated or simple PID controller is used, while the proposed one successfully fulfills it.

TABLE I  
COMPARISON OF TRACKING ERRORS OBTAINED BY CONTROLLERS DURING TORQUE TRANSMISSION

	Proposed controller		Sliding mode controller		PID controller	
	RMS error	Max error	RMS error	Max error	RMS error	Max error
Position [rad]	0.706 (0.74%)	5.428 (5.65%)	1.235 (1.29%)	10.992 (11.5%)	2.065 (2.18%)	15.743 (16.4%)
Torque [N.m]	0.950 (1.58%)	5.525 (9.21%)	1.576 (2.63%)	10.643 (17.7%)	1.729 (2.88%)	11.843 (19.7%)

### B. Adaptive Desired Position Correction

To test the performance of the torque-monitoring controller integrated with the adaptive desired position correction algorithm, the entire system, which consists of the torque observer, sliding mode actuator position tracking controller, and adaptive scheme, is used in the combined manner to control the clutch engagement in the driveline test bench equipped with DCT. Experiment scenarios cover launch, acceleration, upshift, engine braking, power-off downshift, and neutral states.

The main purpose of using the adaptive scheme is to compensate for the varying friction property, which may arise due to the unaccounted change in the hardware properties, temperature, or clutch wear characteristics. However, such condition with vast amount of change in the friction property

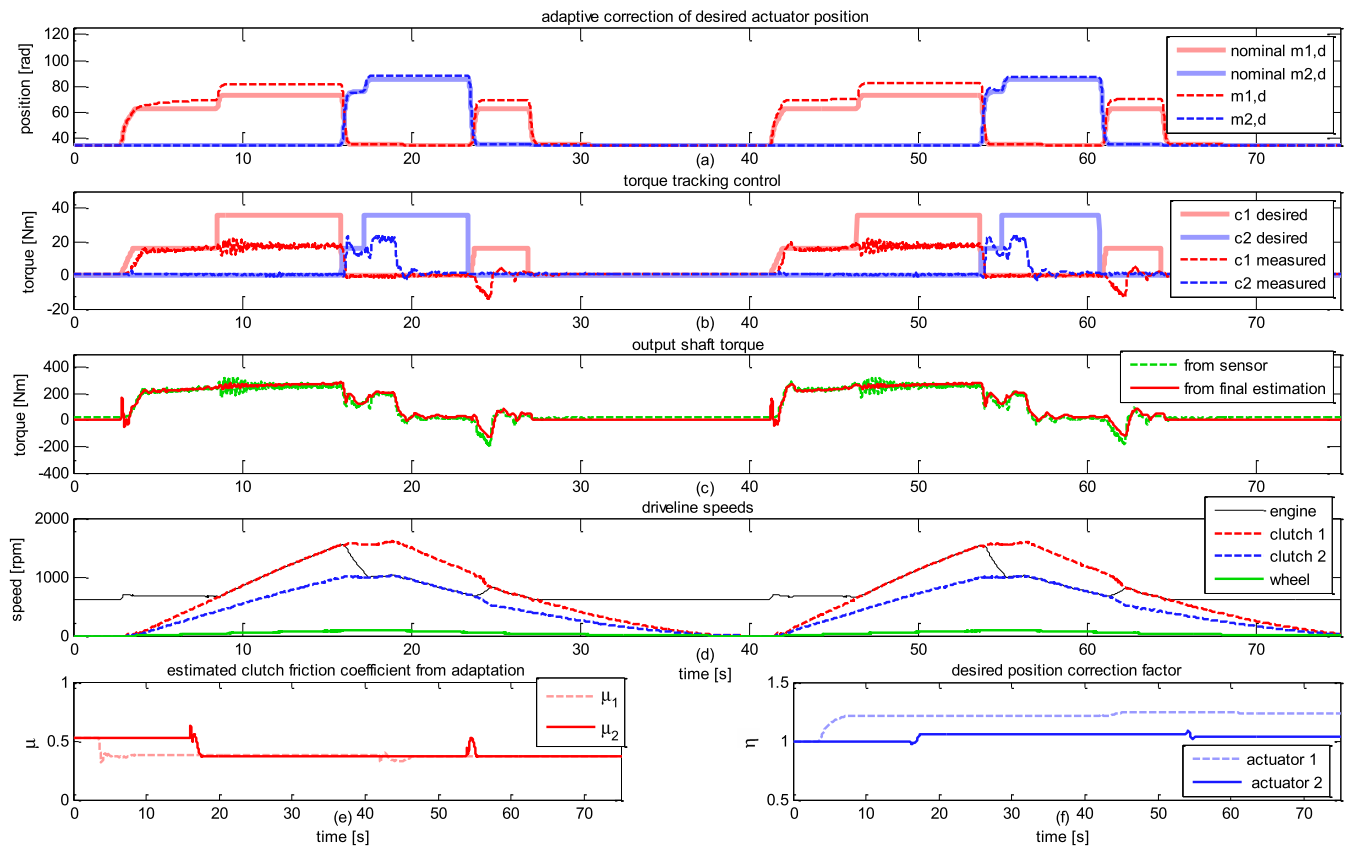


Fig. 7. Experiment results obtained by using the proposed integrated controller with overestimated clutch parameter. (a) Adaptive correction of desired actuator position. (b) Torque tracking control. (c) Output shaft torque. (d) Driveline speeds.

or temperature cannot be created in the test facility due to technical and safety issues. Hence, we chose to intentionally change the nominal value for friction coefficient used in the controller system instead, so that the control performance can be assessed under the effect of obvious discrepancy between the nominal and actual friction properties. The nominal clutch friction coefficient is decreased by 50% from the actual value ( $\mu = 0.35$ ) in case of the underestimated parameter, and is increased by 50% from the actual value in case of the overestimated parameter.

We are interested in the torque-tracking performance during the slipping state of the clutch, because the amount of torque transmission during the locked state of the clutch depends on the engine rather than the clutch engagement control.

The results for the experiment conducted with underestimated clutch friction coefficient are shown in Fig. 6, and those with overestimated clutch friction coefficient are shown in Fig. 7.

In the case of underestimated friction, since the actual friction coefficient is higher than nominal value, clutches are engaged with excessive engaging force that higher torque than desired is transferred as shown in the torque plot during the first launch and first upshift displayed in Fig. 6.

However, Fig. 6(e) and (f) indicates that the adaptive algorithm successfully identifies the correct friction coefficient immediately, so that the correction factor for desired actuator position command can be altered accordingly. The rescaled desired positions are shown in Fig. 6(a), and it can

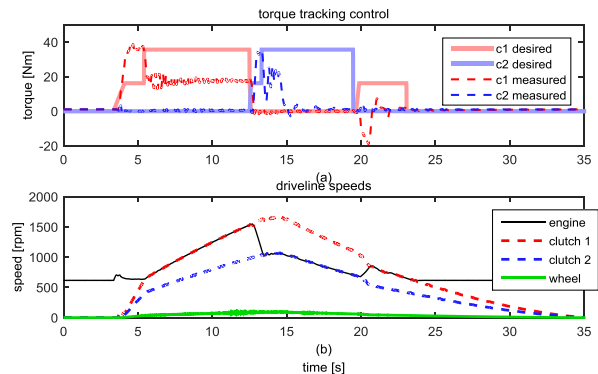


Fig. 8. Experiment results obtained without using adaptive correction when clutch parameter is underestimated. (a) Torque tracking control. (b) Driveline speeds.

be checked that the desired position is decreased quickly to reduce the magnitude of the overshoot. With the adaptive states converged, the actuator now performs with correct clutch parameter to effectively follow the desired torque command in the second trial. Here, plot of the estimated friction coefficients is obtained from the adaptive states  $C_{c1}$  and  $C_{c2}$ .

The adaptive scheme works similarly in the case of overestimated friction. For the first trial in Fig. 7 to engage the clutch during launch and upshift, since the actual friction coefficient is lower than the nominal value, clutches are engaged with insufficient engaging force, and lower torque than desired is transferred. However, the adaptive scheme successfully

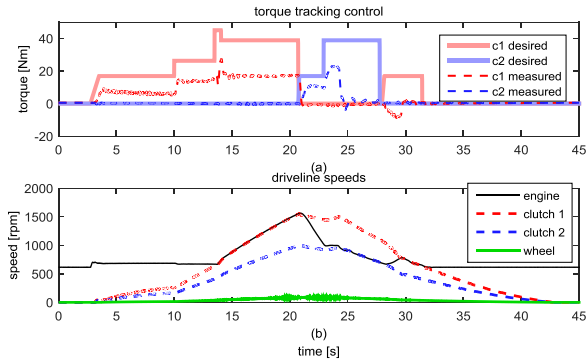


Fig. 9. Experiment results obtained without using adaptive correction when clutch parameter is overestimated. (a) Torque tracking control. (b) Driveline speeds.

TABLE II

COMPARISON OF rms ON-COMING CLUTCH TORQUE TRACKING ERROR

Scenario	launch	upshift	downshift
nominal $\mu = \text{actual } \mu = 0.35$	1.68	4.86	3.40
nominal $\mu = 0.17$ & proposed	1.78	4.21	2.92
nominal $\mu = 0.52$ & proposed	1.44	5.63	3.56
nominal $\mu = 0.17$ & position-based	10.39	12.21	4.33
nominal $\mu = 0.52$ & position-based	9.80	10.12	6.02

converges to the correct parameter and rescales the desired actuator position, so that the clutch effectively transfers the desired amount of torque, immediately after insufficient torque is detected by the torque observer. Then, during the second trial, the controller manages to show satisfactory tracking performance during the entire tested interval.

The convergence of the adaptive states is shown in Figs. 6(e) and (f) and 7 for different cases of initial parameter value. It can be seen here that regardless of the initial nominal clutch parameter, the adaptive scheme effectively manages to converge to the actual ones.

Furthermore, experiments for both underestimated and overestimated friction coefficients are conducted without using the adaptive scheme, and their results are shown in Figs. 8 and 9. As expected, in case of the underestimated friction coefficient, overshoots in the transferred torques are caused to a greater degree than those in the first trial of Fig. 6. Moreover, in case of the overestimated friction coefficient, clutches even fail to engage.

Since the main purpose of the proposed controller is in the improvement of torque-tracking accuracy, the rms torque tracking error is compared as the performance index in Table II. Because the on-coming clutch has dominant influence on the slip-phase torque transmission, the on-coming clutch torque tracking error was chosen as the performance index. As shown here, the proposed controller applied to the cases with incorrect nominal parameters manages to achieve the similar level of performance index to that achieved with the correct parameter.

## V. CONCLUSION

This brief has proposed a novel controller algorithm based on the torque-monitoring strategy, which is aimed for

TABLE III  
PARAMETERS AND TUNING GAINS

Parameter	Value	Parameter	Value
$L_m$	0.4mH	$T_{c,threshold}$	20 N.m
$k_{emf}$	0.016 V·s/rad	$\lambda$	11
$k_a$	0.016 N·m/A	$\gamma_s$	$5 \times 10^3$
$R_m$	0.9 $\Omega$	$\gamma_z$	100
$J_a^*$	$4 \times 10^{-3}$ kg·m <sup>2</sup>	$\gamma_{a1}$	0.05
$r_p$	0.095 m	$\gamma_{a2}$	1
$R_c$	0.095 m	$\gamma_n$	0.08
$N_{ae}$	944		

effectively tracking the desired clutch torque command in DCT with the SECA system. Summarizing this brief, the noteworthy contribution served by this brief is twofold: the sliding mode actuator position tracking controller and adaptive desired position correction. By utilizing the torque estimations obtained by the torque observer, the proposed sliding mode tracking controller has its advantage in the ability to reduce both steady state and transient tracking error when applied to the SECA. The adaptive desired position correction has the unique advantage in improving the clutch torque tracking control performance even under the influence of uncertainty in the clutch model parameters. These original contributions are thoroughly verified through theoretical stability analysis and actual test bench experiments. With the application of the proposed work on actual vehicle driveline, improved control precision and actuator efficiency can be anticipated.

## APPENDIX

See Table III.

## REFERENCES

- [1] L. Glielmo, L. Iannelli, V. Vacca, and F. Vasca, "Gearshift control for automated manual transmissions," *IEEE/ASME Trans. Mechatronics*, vol. 11, no. 1, pp. 17–26, Feb. 2006.
- [2] M. Pisaturo, M. Cirrincione, and A. Senatore, "Multiple constrained MPC design for automotive dry clutch engagement," *IEEE/ASME Trans. Mechatronics*, vol. 20, no. 1, pp. 469–480, Feb. 2015.
- [3] T. Hofman, S. Ebbesen, and L. Guzzella, "Topology optimization for hybrid electric vehicles with automated transmissions," *IEEE Trans. Veh. Technol.*, vol. 61, no. 6, pp. 2442–2451, Jul. 2012.
- [4] K. Zhao, Y. Liu, X. Huang, R. Yang, and J. Wei, "Uninterrupted shift transmission and its shift characteristics," *IEEE/ASME Trans. Mechatronics*, vol. 19, no. 1, pp. 374–383, Feb. 2014.
- [5] B. Matthes, "Dual clutch transmissions—Lessons learned and future potential," SAE Tech. Paper 2005-01-1021, 2005.
- [6] J. Kim and S. B. Choi, "Design and modeling of a clutch actuator system with self-energizing mechanism," *IEEE/ASME Trans. Mechatronics*, vol. 16, no. 5, pp. 953–966, Oct. 2011.
- [7] C. Ni, T. Lu, and J. Zhang, "Gearshift control for dry dual-clutch transmissions," *WSEAS Trans. Syst.*, vol. 8, no. 11, pp. 1177–1186, 2009.
- [8] K. van Berkel, F. Veldpaus, T. Hofman, B. Vroemen, and M. Steinbuch, "Fast and smooth clutch engagement control for a mechanical hybrid powertrain," *IEEE Trans. Control Syst. Technol.*, vol. 22, no. 4, pp. 1241–1254, Jul. 2014.
- [9] O. Sundstrom, P. Soltic, and L. Guzzella, "A transmission-actuated energy-management strategy," *IEEE Trans. Veh. Technol.*, vol. 59, no. 1, pp. 84–92, Jan. 2010.
- [10] S. J. Kim, Y.-S. Yoon, S. Kim, and K.-S. Kim, "Fuel economy assessment of novel multi-mode parallel hybrid electric vehicle," *Int. J. Autom. Technol.*, vol. 16, no. 3, pp. 501–512, 2015.

- [11] W. Zhuang, X. Zhang, D. Zhao, H. Peng, and L. Wang, "Optimal design of three-planetary-gear power-split hybrid powertrains," *Int. J. Autom. Technol.*, vol. 17, no. 2, pp. 299–309, 2016.
- [12] A. Grancharova and T. A. Johansen, "Design and comparison of explicit model predictive controllers for an electropneumatic clutch actuator using on/off valves," *IEEE/ASME Trans. Mechatronics*, vol. 16, no. 4, pp. 665–673, Aug. 2011.
- [13] J. Deur, V. Ivanović, Z. Herold, M. Kostelac, and H. E. Tseng, "Dry clutch control based on electromechanical actuator position feedback loop," *Int. J. Vehicle Design*, vol. 60, no. 3, pp. 305–326, 2012.
- [14] F. Vasca, L. Iannelli, A. Senatore, and G. Reale, "Torque transmissibility assessment for automotive dry-clutch engagement," *IEEE/ASME Trans. Mechatronics*, vol. 16, no. 3, pp. 564–573, Jun. 2011.
- [15] A. Myklebust and L. Eriksson, "Modeling, observability, and estimation of thermal effects and aging on transmitted torque in a heavy duty truck with a dry clutch," *IEEE/ASME Trans. Mechatronics*, vol. 20, no. 1, pp. 61–72, Feb. 2015.
- [16] G. Pica, C. Cervone, A. Senatore, and F. Vasca, "Temperature-dependent torque transmissibility characteristic for automotive dry dual clutches," in *Proc. Eur. Control Conf. (ECC)*, 2015, pp. 2126–2131.
- [17] M. Kulkarni, T. Shim, and Y. Zhang, "Shift dynamics and control of dual-clutch transmissions," *Mech. Mach. Theory*, vol. 42, no. 2, pp. 168–182, 2007.
- [18] P. D. Walker, N. Zhang, and R. Tamba, "Control of gear shifts in dual clutch transmission powertrains," *Mech. Syst. Signal Process.*, vol. 25, no. 6, pp. 1923–1936, 2011.
- [19] M. Goetz, M. C. Levesley, and D. A. Crolla, "Dynamics and control of gearshifts on twin-clutch transmissions," *Proc. Inst. Mech. Eng. D, J. Automobile Eng.*, vol. 219, no. 8, pp. 951–963, 2005.
- [20] J. Oh, S. B. Choi, Y. J. Chang, and J. S. Eo, "Engine clutch torque estimation for parallel-type hybrid electric vehicles," *Int. J. Autom. Technol.*, vol. 18, no. 1, pp. 125–135, 2017.
- [21] G. Shi, P. Dong, H. Q. Sun, Y. Liu, Y. J. Cheng, and X. Y. Xu, "Adaptive control of the shifting process in automatic transmissions," *Int. J. Autom. Technol.*, vol. 18, no. 1, pp. 179–194, 2017.
- [22] L. Glielmo, L. Iannelli, V. Vacca, and F. Vasca, "Speed control for automated manual transmission with dry clutch," in *Proc. 43rd IEEE Conf. Decision Control (CDC)*, vol. 2, Dec. 2014, pp. 1709–1714.
- [23] J. J. Oh and S. B. Choi, "Real-time estimation of transmitted torque on each clutch for ground vehicles with dual clutch transmission," *IEEE/ASME Trans. Mechatronics*, vol. 20, no. 1, pp. 24–36, Feb. 2015.
- [24] R. Roberts, M. Schautt, H. Hartmann, and B. Gombert, "Modeling and validation of the mechatronic wedge brake," SAE Tech. Paper 2003-01-3331, 2003.
- [25] L. Balogh, T. Strelci, H. Nemeth, and L. Palkovics, "Modelling and simulating of self-energizing brake system," *Vehicle Syst. Dyn.*, vol. 44, no. 1, pp. 368–377, 2006.
- [26] H. Park and S. B. Choi, "Development of a sensorless control method for a self-energizing brake system using noncircular gears," *IEEE Trans. Control Syst. Technol.*, vol. 21, no. 4, pp. 1328–1339, Jul. 2013.
- [27] S. S. Rao and L. Cao, "Optimum design of mechanical systems involving interval parameters," *J. Mech. Des.*, vol. 124, no. 3, pp. 465–472, 2002.
- [28] Y. M. Huang and J. S. Shyr, "On pressure distributions of drum brakes," *J. Mech. Des.*, vol. 124, no. 1, pp. 115–120, 2002.
- [29] C. C. de Wit, H. Olsson, K. J. Åström, and P. Lischinsky, "A new model for control of systems with friction," *IEEE Trans. Autom. Control*, vol. 40, no. 3, pp. 419–425, Mar. 1995.
- [30] P. A. Ioannou and J. Sun, *Robust Adaptive Control*. Englewood Cliffs, NJ, USA: Prentice-Hall, 1964, p. 150.
- [31] J. E. Slotine and W. Li, *Applied Nonlinear Control*. Englewood Cliffs, NJ, USA: Prentice-Hall, 1991.